Evidence for shallow implantation during the growth of bismuth nanocrystals by pulsed laser deposition

J-P. Barnes, A. K. Petford-Long, A. Suárez-García, and R. Serna

Citation: J. Appl. Phys. **93**, 6396 (2003); doi: 10.1063/1.1564878

View online: http://dx.doi.org/10.1063/1.1564878

View Table of Contents: http://jap.aip.org/resource/1/JAPIAU/v93/i10

Published by the American Institute of Physics.

Evidence for shallow implantation during the growth of bismuth nanocrystals by pulsed laser deposition

J-P. Barnes[a] and A. K. Petford-Long
Department of Materials, Oxford University, Parks Road, Oxford, OX1 3PH, England

A. Suárez-García and R. Serna
Instituto de Optica, C.S.I.C., Serrano 121, 28006, Madrid, Spain

(Received 12 August 2002; accepted 5 February 2003)

The implantation of bismuth during pulsed laser deposition (PLD) has been directly observed and investigated. Bi was deposited on amorphous aluminum oxide (Al_2O_3) and the laser energy density on the Bi target was varied by one order of magnitude (0.4 to 5 $J\,cm^{-2}$). Cross-sectional transmission electron micrographs reveal that, for laser energy densities above 2 $J\,cm^{-2}$, in addition to the formation of Bi nanocrystals, there is a dark and apparently continuous layer in the Al_2O_3 underneath them. From previous velocity measurements, the kinetic energy of the Bi species in the plume generated at laser energy densities above 2 $J\,cm^{-2}$ has been estimated to be around 200 eV, which gives a calculated implantation range of 1.8 nm in Al_2O_3. This is in good agreement with the position of the Bi-rich layer. © *2003 American Institute of Physics.* [DOI: 10.1063/1.1564878]

There is considerable interest in nanocomposites of metal nanocrystals (NCs) embedded in an oxide matrix because they can show a wide range of interesting mechanical, catalytic, electrical, and optical properties. Thus, synthesis methods that allow the growth of good-quality oxides and the development of well-controlled metal NCs are required. Pulsed laser deposition (PLD) is a thin-film deposition technique that is especially suited for the deposition of complex oxides.[1,2] In previous work we have shown the potential of PLD for the growth of metal NCs (Cu, Bi, Ag) embedded in amorphous aluminum oxide (Al_2O_3),[3–7] and how the NC size, shape, and distribution can be modified as a function of the number of pulses on the metal target. The influence of the energy density used for ablation has not been studied in detail, although it is expected to have a significant influence on the structure of the nanocomposite because of the high-kinetic-energy species (up to several hundred eV) that are present in typical plasmas during PLD. These high-energy species are a key factor in explaining the formation of high-density films with good adhesion by PLD.[1,2] However, they may also result in resputtering of surface atoms and shallow implantation that can cause significant interfacial mixing and the production of metastable phases.[8] These effects are very important whenever artificial structures have to be developed, and have been addressed in the case of multilayer films.[9,10] However, the influence of the high-kinetic-energy species produced during PLD on the growth of metal NCs embedded in an oxide matrix deserves special attention.

The aim of this work is to investigate the influence that the energy density used to ablate the metal target has on the structure of the deposit, and, more specifically, to investigate implantation effects. For this study, Bi has been chosen because it has a low melting point and low thermal conductivity compared to most metals, which allow a wide range of energy densities to be used for ablation. It will be also shown that its high atomic mass provides the Bi species with a high kinetic energy in the PLD plasma as well as providing high contrast relative to the oxide matrix for transmission electron microscope (TEM) observation.

An ArF excimer laser (193-nm, 20-ns full width at half maximum, 5–20-Hz repetition rate) was used to alternately ablate high-purity Al_2O_3 and Bi targets in vacuum (10^{-6} Torr). The substrates were positioned at a distance of 32 mm along the target normal and kept at room temperature. To study the in-plane morphology at different energy densities, simple sandwich structures of Al_2O_3/Bi/Al_2O_3 were grown on carbon-coated mica so as to avoid overlapping images from superimposed NCs when viewed in transmission. The energy density on the Al_2O_3 was kept constant at 5 (± 1) $J\,cm^{-2}$, and an approximate thickness of 10 nm of Al_2O_3 was deposited before and after the Bi NCs. The energy density used to ablate the Bi target was varied using an attenuator in the laser beam path before the focusing lens. Three samples were grown with energy densities of 0.4 (± 0.1) $J\,cm^{-2}$, 2 (± 0.4) $J\,cm^{-2}$, and 5 (± 1) $J\,cm^{-2}$ on the Bi target. The lowest energy density was close to the Bi ablation threshold. The Bi content of each deposit was kept constant, by choosing an appropriate number of pulses on the target, and it was checked after deposition using Rutherford backscattering spectroscopy. A 2.0-MeV $^4He^+$ beam was used and the experimental spectra were analyzed using the RUMP code.[11] The total areal density of the Bi deposits was found to be $1.9 \pm 0.5 \times 10^{15}$ atoms cm^{-2}. TEM analysis of the film structure was carried out using a JEOL 4000EX operated at 400 kV with a point- to-point resolution of 0.16 nm.

Figure 1 shows plan-view images corresponding to the films deposited at the lowest and the highest energy densities. The Bi NCs are imaged as dark areas on a lighter background, which correspond to the amorphous Al_2O_3. Size distributions are included beside each image which show no

[a]Electronic mail: jean-paul.barnes@materials.ox.ac.uk

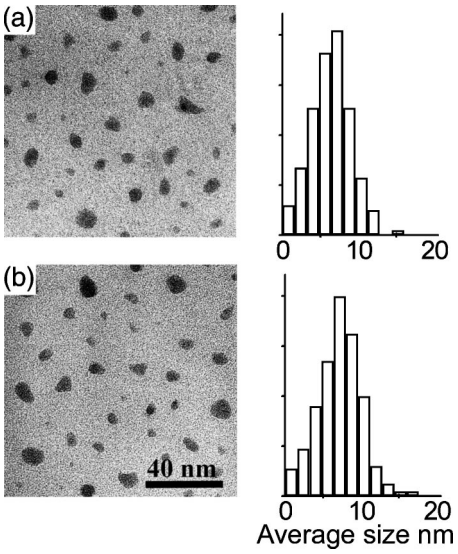

FIG. 1. Plan-view TEM images with corresponding average in-plane size distributions of Bi deposited at (a) 5 J cm^{-2} and (b) 0.4 J cm^{-2}.

significant dependence of the in-plane morphology of the NCs on the change in energy density. The average NC diameters from highest to lowest energy density are 6.4 ($\pm$0.6), 6.9 ($\pm$0.6), and 7.2 ($\pm$0.6) nm, with standard deviations for the size distribution of 2.7, 2.8, and 3.0 nm respectively. The variation in mean diameter with energy density is within the expected range, given the error in calibrating the deposition rate at the different energy densities, which results in slight variations in the exact amount of Bi deposited.

In order to study the morphology of the NCs in the direction normal to the film plane, a single sample containing three layers of Bi NCs, each grown at one of the three different energy densities, was deposited on a silicon substrate so that a cross-sectional sample could be prepared. The deposition sequence starting from the Si substrate was Al_2O_3/ Bi(0.4 J cm^{-2})/ Al_2O_3/ Bi(2 J cm^{-2})/ Al_2O_3/ Bi(5 J cm^{-2})/ Al_2O_3 where all the Al_2O_3 layers were grown to have an approximate thickness of 20 nm to ensure that each new Bi NC layer nucleates on a fresh flat surface. The growth of all the Bi NCs layers in one sample enables a direct comparison to be made without artifacts from preparation techniques or TEM observation conditions. The cross-sectional sample was prepared using an FEI 200TEM focused ion beam system and is approximately 40 nm thick.

Figure 2 shows the cross-sectional image. The energy density used to ablate the Bi target to form the NCs increases from bottom to top. The Al_2O_3 layers are very homogeneous and the Al_2O_3 species fill in the spaces between the previously deposited NCs. The NCs in this projection appear either circular or elliptical in shape. As was seen in the plan-view images, there is no significant variation in the morphology of the Bi NCs with the energy density used to ablate the Bi target. The average heights of the NCs are 5.6 ($\pm$0.6), 6.1 ($\pm$0.6), and 6.2 ($\pm$0.6) nm from highest to lowest energy density, respectively, with standard deviations of 1, 0.7, and 1 nm. It is thought that once Bi nuclei are formed on the Al_2O_3 surface, these nuclei grow into three-dimensional islands as more Bi arrives. The characteristics of

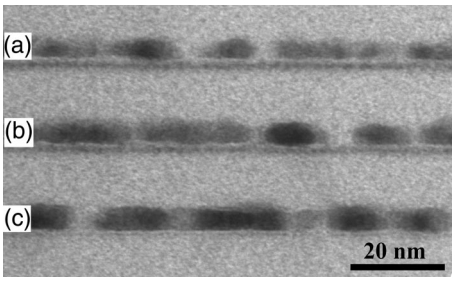

FIG. 2. Cross-sectional TEM image of the multilayer film deposited on Si. The energy density used to deposit the Bi is (a) 5 J cm^{-2}, (b) 2 J cm^{-2}, and (c) 0.4 J cm^{-2}.

the growth appear very similar to our earlier observations for the growth of Cu and Ag NCs in amorphous Al_2O_3.[3,4,7]

The most surprising feature in the cross-sectional image is the continuous layer of dark contrast below the Bi NCs at depths of 1.1 ($\pm$0.3) nm and 1.6 ($\pm$0.3) nm for the depositions at 2 and 5 J cm^{-2}, with layer thicknesses of 1.0 ($\pm$0.3) and 1.3 ($\pm$0.3) nm, respectively. This layer of dark contrast has been confirmed as Bi-rich in composition by energy-dispersive x-ray (EDX) analysis performed in a JEOL 3000F operated at 297 kV with a probe size of less than 1 nm in diameter. No such layer can be seen under the NCs deposited at 0.4 J cm^{-2}. Figure 3 shows a high-resolution electron microscope (HREM) image corresponding to the 2 J cm^{-2} deposition condition. The image shows a large Bi NC in which lattice fringes can be seen, plus several smaller NCs that appear to overlap in this projection. To the left is an area with no nanocrystals, which shows that the Bi-rich layer develops independently of the NCs.

In order to explain the observation of this Bi-rich layer, it is useful to consider the energy of the Bi species arriving at the Al_2O_3 surface. In a previous work using spatially resolved, real-time optical emission spectroscopy and similar energy densities, an expansion velocity of $\approx 1.4\times 10^6$ cm s^{-1} was estimated for the plasma of the excited neutrals and ions (Bi^{+*} and Bi* species).[12] This is equivalent to a kinetic energy of around 200 eV. SRIM software[13] was used to estimate the implantation range for Bi in amorphous Al_2O_3 (density of 2.95 g cm^{-3})[14] with kinetic energies in the range from 0 to 400 eV. The results are plotted in Fig. 4. A kinetic energy of 200 eV can be seen to be sufficient to result in an approximate implantation range of 1.8 nm and a straggle (the standard deviation in the direction of implantation) of 0.4 nm. Given the errors in measuring the depth of the Bi-rich layer, this implantation range compares well with the mean

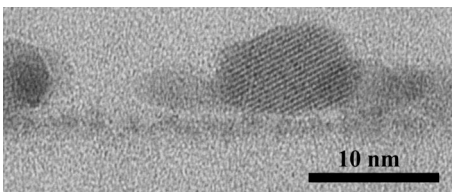

FIG. 3. Cross-sectional HREM image corresponding to the 2 J cm^{-2} density deposition energy.

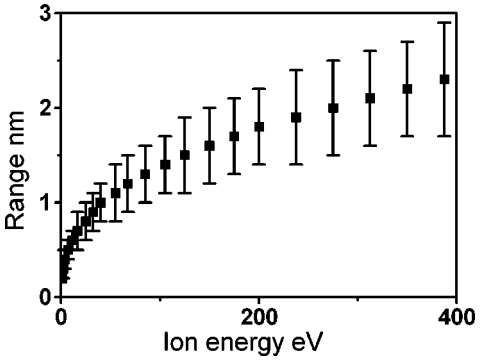

FIG. 4. Bi ion implantation range against ion energy. The error bars correspond to longitudinal straggle.

distance below the surface at which the Bi rich layer is observed in the cross-sectional image of the Bi deposited at 2 and 5 $J\,cm^{-2}$.

The decrease in the depth of the Bi-rich layer from 1.6 to 1.1 nm on reducing the energy density from 5 to 2 $J\,cm^{-2}$ suggests that a further decrease in the implantation depth should be expected on decreasing the energy density to 0.4 $J\,cm^{-2}$. Assuming that in the range of energy densities used, the kinetic energy of the ablated species have a linear dependence on energy density, an implantation depth of 0.5 nm or less would be expected.[15] This would not only be difficult to see in the TEM image, but any implanted species might also diffuse back to the surface. This agrees with the absence of a clearly visible Bi-rich layer for an energy density of 0.4 $J\,cm^{-2}$. Therefore, it can be concluded that the Bi-rich layer beneath the NCs is formed by the high-kinetic-energy Bi species present in the plasma. The Bi implantation is probably initiated at the start of the deposition process, and it might influence the nucleation of the NCs by modifying the surface of the Al_2O_3.

It is interesting to note that studies of plasma expansion dynamics performed in several PLD systems show that for energy densities around 2 $J\,cm^{-2}$, the expansion velocities of the studied species are in the range of 10^6 $cm\,s^{-1}$, irrespective of the target material.[1,12,15,16] Therefore, the kinetic energy will depend predominantly on the atomic mass. Hence, the lighter the element, the shorter the expected implantation range. For two other metals that we have used to grow NCs—Cu ($m_a = 63.5$ amu) and Ag ($m_a = 108$)—the kinetic energies would be about three and two times less than that of Bi, respectively. This means an implantation range of only 0.5 nm for Cu, which would be difficult to observe. For Ag, an implantation range of about 0.8 nm is estimated, which agrees with the recent observation of a faint underlayer very close to the Ag NCs.[7] Nevertheless, even for this case, the implantation effect is important, although it may more often be described as mixing at the interface with the previously deposited material, as has been reported for metal multilayers such as Fe/Ag.[8–10]

The presence of the layer is likely to have a significant effect on the optical properties of the nanocomposite. The inclusion of small amounts of metal ions can significantly increase the refractive index of the oxide matrix,[5,17] thus affecting the position of the surface plasmon resonance.[18] The electric and magnetic properties might be also affected. For example, in the case of composites of Fe nanocrystals in amorphous Al_2O_3 grown by PLD, significant modifications in the magneto-optical response have been reported when the presence of dissolved Fe atoms in the dielectric matrix is taken into account.[19]

In conclusion, during PLD of Bi on Al_2O_3, the shallow implantation of Bi species has been shown for energy densities above 2 $J\,cm^{-2}$. The implantation range has been shown to depend on the energy density used for ablation, which is related to the velocity of the Bi atoms and ions in the plasma. It has been highlighted that implantation during PLD is more likely the higher the mass of the ablated species, based on previous measurements that have shown that there is no significant dependence of expansion velocity on the metal chosen for ablation. Further studies are needed to determine in detail the velocity distribution of the ablated species, and to analyze the effect that such an implanted layer has on the electrical, magnetic, and optical properties of the nanocomposite.

ACKNOWLEDGMENTS

D. Hole is acknowledged for performing Rutherford backscattering measurements and R. C. Doole for obtaining EDX analysis. We would especially like to thank Dr. C. N. Afonso for helpful discussion and suggestions. This work has been partially supported by project TIC99-0866, CICYT (Spain). One of the authors (J.-P.B.) acknowledges support by the EPSRC and a Marie Curie Fellowship of the EC under Contract No. HPMT-CT-2000-00064.

[1] *Pulsed Laser Deposition of Thin Films*, edited by D. B. Chrisey and G. K. Hubler (Wiley, New York, 1994).
[2] C. N. Afonso, in *Insulating Materials for Optoelectronics* (World Scientific, Singapore, 1995), Chap. 1.
[3] J. M. Ballesteros, R. Serna, J. Solís, C. N. Afonso, A. K. Petford-Long, D. H. Osborne, and R. F. Haglund, Jr., Appl. Phys. Lett. **71**, 2445 (1997).
[4] R. Serna, J. Gonzalo, A. Suárez-García, C. N. Afonso, J. P. Barnes, A. K. Petford-Long, R. C. Doole, and D. Hole, J. Microsc. **201**, 250 (2001).
[5] R. Serna, J. C. G. de Sande, J. M. Ballesteros, and C. N. Afonso, J. Appl. Phys. **84**, 4509 (1998).
[6] J. C. G. de Sande, R. Serna, J. Gonzalo, C. N. Afonso, D. E. Hole, and A. Naudon, J. Appl. Phys. **91**, 1536 (2002).
[7] J. P. Barnes, A. K. Petford-Long, R. C. Doole, R. Serna, J. Gonzalo, A. Suárez-García, C. N. Afonso, and D. Hole, Nanotechnology **13**, 465 (2002).
[8] S. Fahler, S. Khal, M. Weisheit, K. Sturm, and H. U. Krebs, Appl. Surf. Sci. **154–155**, 419 (2000).
[9] H. U. Krebs, M. Stormer, S. Fahler, O. Bremert, M. Hamp, A. Pundt, H. Teichler, W. Blum, and T. H. Metzger, Appl. Surf. Sci. **109**, 563 (1997).
[10] K. Sturm and H. U. Krebs, J. Appl. Phys. **90**, 1061 (2001).
[11] L. R. Doolitle, Nucl. Instrum. Methods Phys. Res. B **9**, 344 (1985).
[12] J. Gonzalo, J. M. Ballesteros, and C. N. Afonso, Appl. Surf. Sci. **138–139**, 52 (1999).
[13] J. F. Ziegler, J. P. Biersack, and U. Littmark, *The Stopping and Range of Ions in Solids* (Pergamon, New York, 1985).
[14] R. Serna, J. C. G. de Sande, J. M. Ballesteros, and C. N. Afonso, J. Appl. Phys. **84**, 4509 (1998).
[15] R. J. von Gurtfeld and R. W. Dreyfus, Appl. Phys. Lett. **54**, 1212 (1989).
[16] J. Gonzalo, C. N. Afonso, and I. Madariaga, J. Appl. Phys. **81**, 951 (1997).
[17] F. Gonella, Appl. Phys. Lett. **69**, 314 (1996).
[18] U. Kreibig and M. Vollmer, *Optical Properties of Metal Clusters* (Springer, Berlin, 1995), Chap. 2, pp. 83–84.
[19] J. L. Menéndez, B. Bescós, G. Armelles, A. Cebollada, R. Serna, J. Gonzalo, R. Doole, and A. K. Petford-Long, Phys. Rev. B **65**, 205413 (2002).